coqusy/06

Electronic properties of curved graphene sheets

Alberto Cortijo, María A. H. Vozmediano
Universidad Carlos III de Madrid-ICMM

Outline

1. Disorder in graphene. Observations.
2. Topological defects.
3. A cosmological model.
4. Effect on the density of states.
5. Summary and future.

Collaborators

Instituto de Ciencia de Materiales de Madrid
(Theory group)

Paco Guinea
José González

Belén Valenzuela
Alberto Cortijo

Pilar López-Sancho
Tobias Stauber

Observation of topological defects in graphene

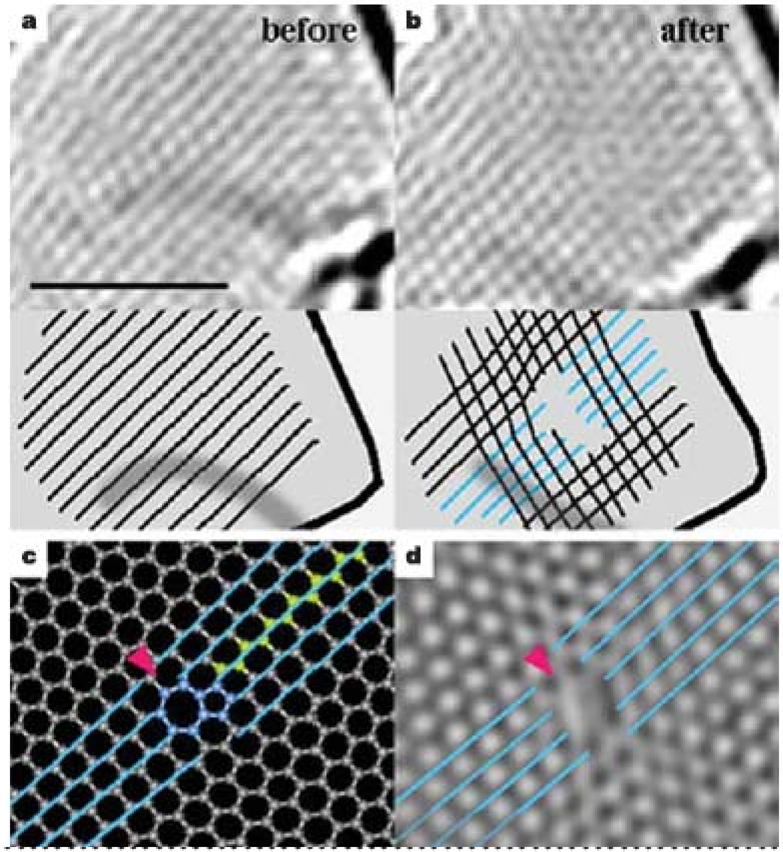

NATURE | VOL 430 | 19 AUGUST 2004 |

Direct evidence for atomic defects in graphene layers

Ayako Hashimoto[1], Kazu Suenaga[1], Alexandre Gloter[1,2], Koki Urita[1,3] & Sumio Iijima[1]

Defects must be present in all graphene samples and have a strong influence on the electronic properties

Vacancies
Ad-atoms
Edges
Topological defects

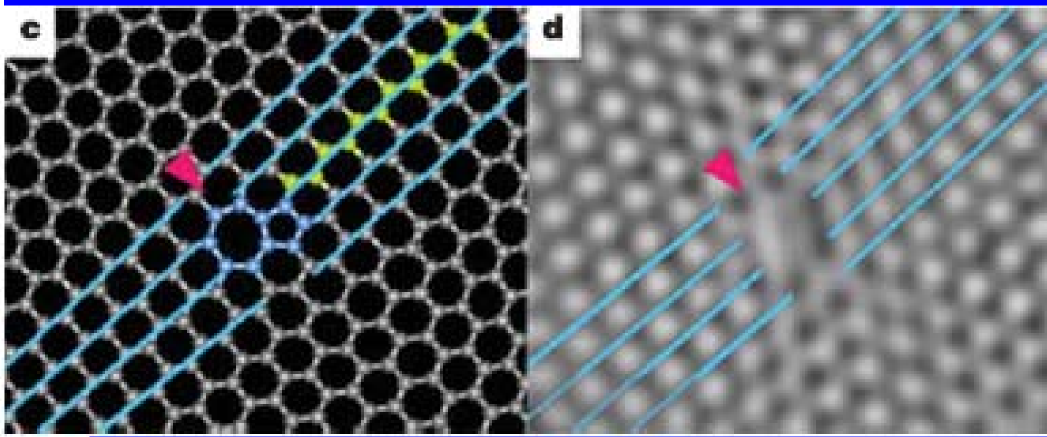

In situ of defect formation in single graphene layers by high-resolution TEM.

Observation of cones of various deficit angles

Graphitic cones and the nucleation of curved carbon surfaces

A. Krishnan*, E. Dujardin†, M. M. J. Treacy*, J. Hugdahl‡, S. Lynum‡ & T. W. Ebbesen*§

NATURE | VOL 388 | 31 JULY 1997

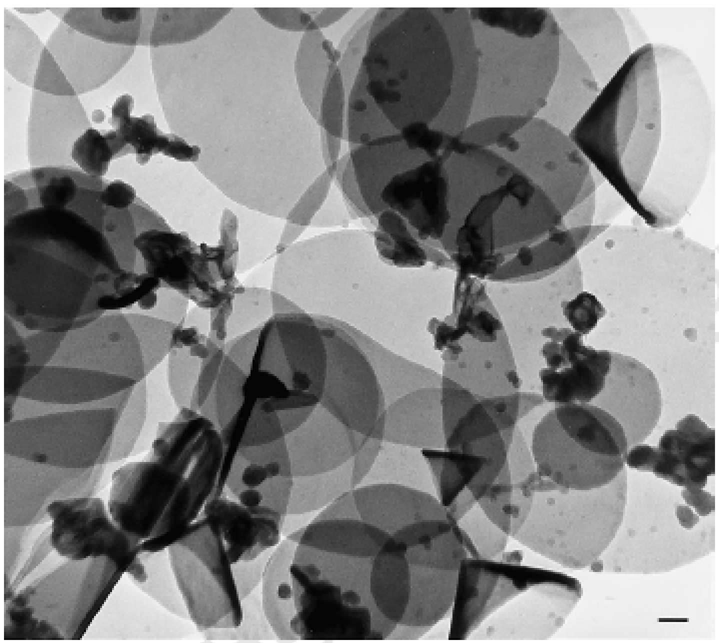

Transmission electron micrograph of the microstructures in the sample.
Scale bar 200nm

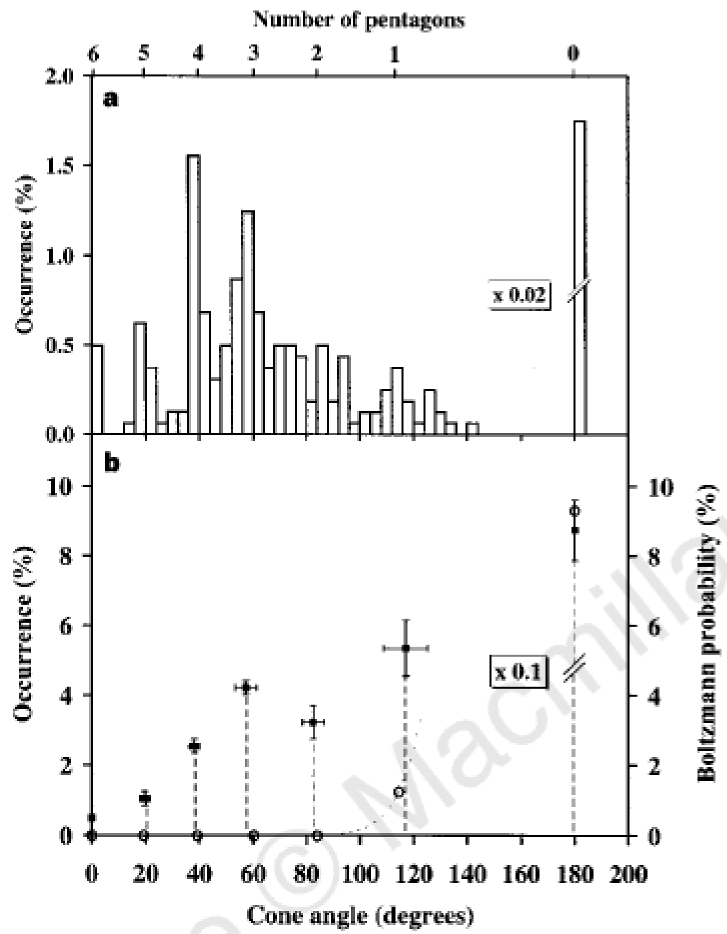

Figure 3 a, Statistical distribution of the measured cone angles among the microstructures; **b**, averaged distribution centred at the seven possible disclinations. The open circles and dotted line represent the calculated Boltzmann distribution of microstructures for a temperature of 2,000 °C and a pentagon energy of formation of 0.75 eV (ref. 19).

Naturally occurring graphite cones

J. A. Jaszczaka et al. **Carbon 03**

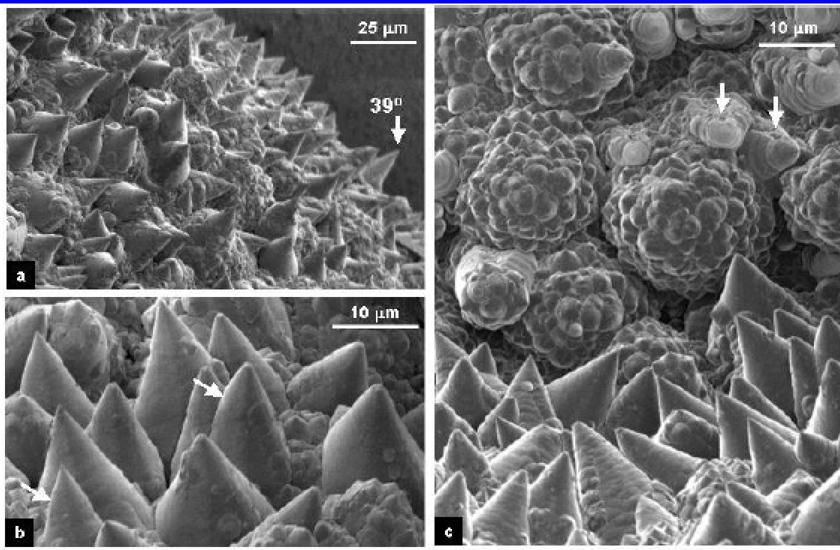

Fig. 2. FESEM images of a cone-covered graphite aggregate. (a) Low-magnification image showing complete coverage of the aggregate surface with conical structures. A ~39° cone is marked by an arrow. (b) Higher magnification image of the sample showing a variety of large cones with different apex angles and sharp and blunt tips. Arrows show changes in the apex angle. (c) Close up view of two surfaces which are almost perpendicular and show different cone morphologies – large cones on one surface and globular (artichoke-like) structures on the other. The latter ones are clusters of large-angle cones. Arrows show some of the cones that are ripped on the side

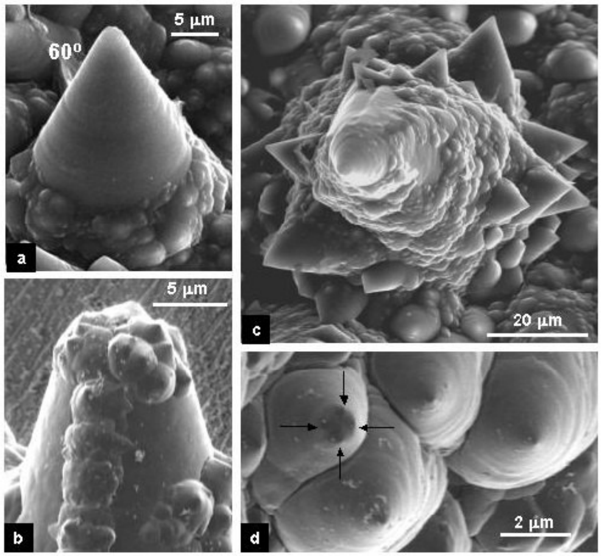

Fig. 3. Typical cone morphologies. (a) SEM image of a cone with a 60° apex angle, the most common apex angle. The slightly uneven surface of the cone suggests layer growth. (b) FESEM and (c) SEM images of large cones with numerous smaller cones growing on their surface. Smaller cones covering surfaces of large cones have a broad distribution of shapes, but large apex angles prevail (c). (d) FESEM image of four cones having sharp and broad tips (multiple tips are marked by arrows). The cones are oriented to reveal their circular cross sections around the tips and layered growth (ripples).

The cone morphologies, which are extremely rare in the mineral and material kingdom, can dominate the graphite surfaces.

Observation of a single pentagon in graphene

Appl. Phys. Lett., Vol. 78, No. 23, 4 June 2001

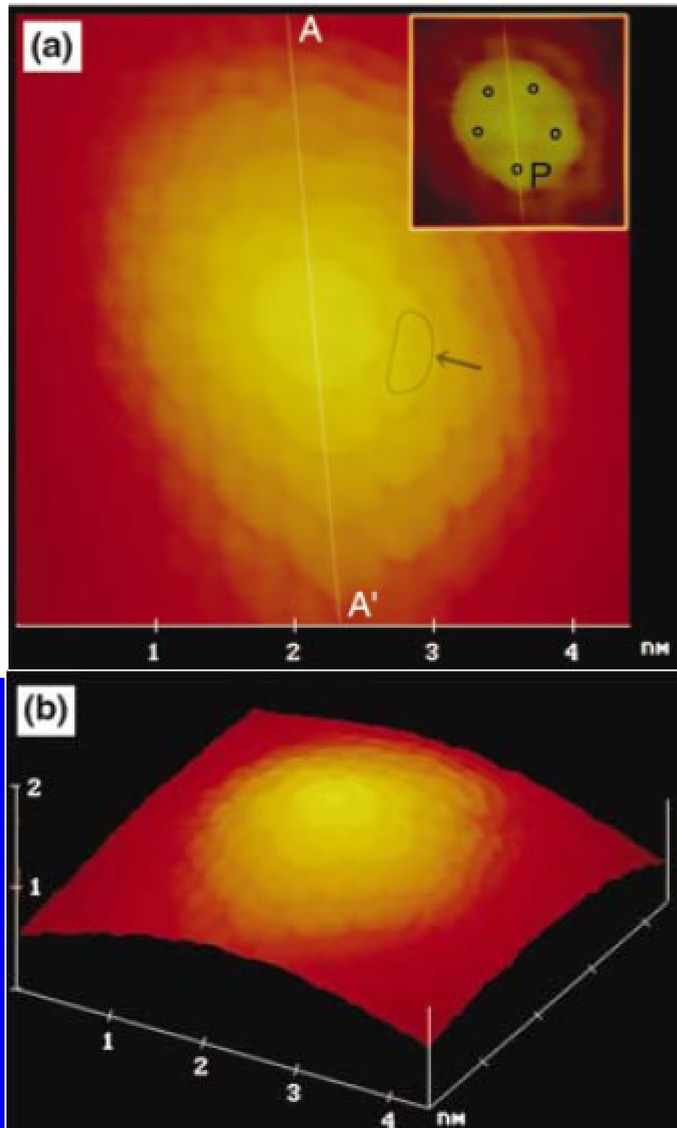

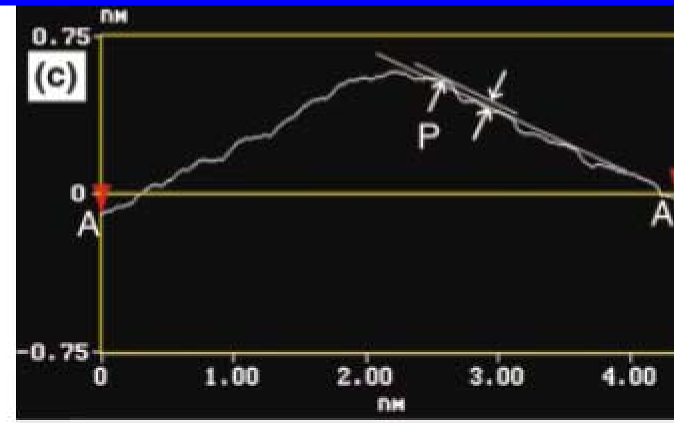

FIG. 2. (Color) Typical images of the conical protuberance by STM. (a) Top view of the apex in 4.4 nm×4.4 nm using a sample bias of 50 mV and tunneling current of 1.0 nA. (b) Bird's-eye view of (a). (c) Cross section along line AA' passing through one of the five bright spots (P) and their center in (a).

Single pentagon in a hexagonal carbon lattice revealed by scanning tunneling microscopy. B. An, S. Fukuyama, et. al.

Stone-Wales defect

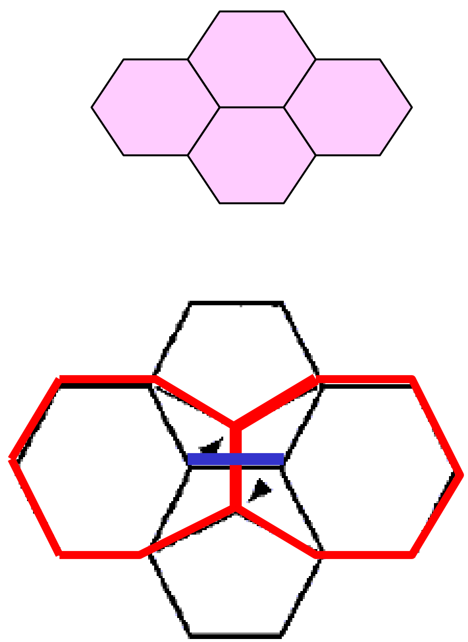

- A 90 degrees local bond rotation in a graphitic network leads to the formation of two heptagons and two pentagons
- Static (dynamic) activation barrier for formation 8-12 (3.6) eV in SWCNs

Formation of pentagonal defects in graphene

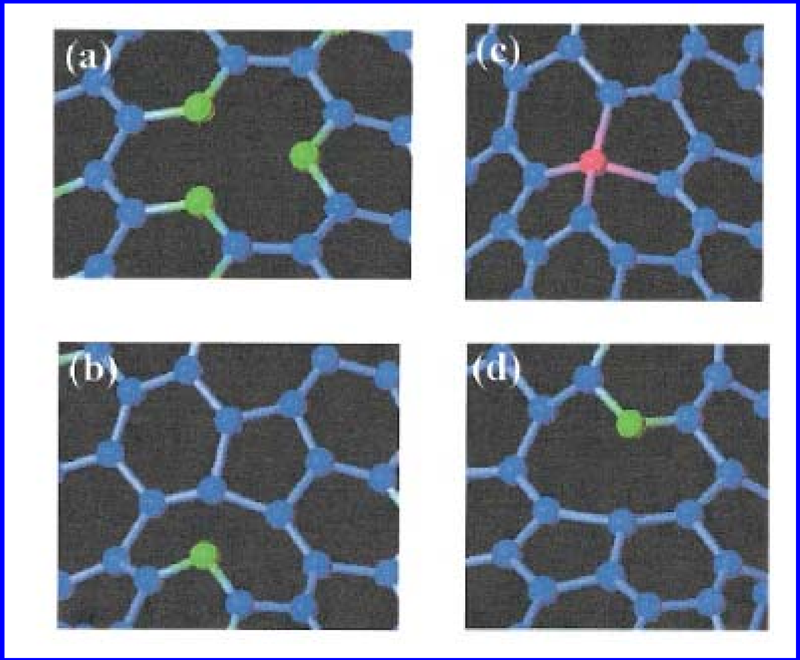

In the .pentagon road model pentagons are formed in seed structures in order to eliminate high-energy dangling bonds, and as an annealing mechanism to reduce the overall energy of the structure.

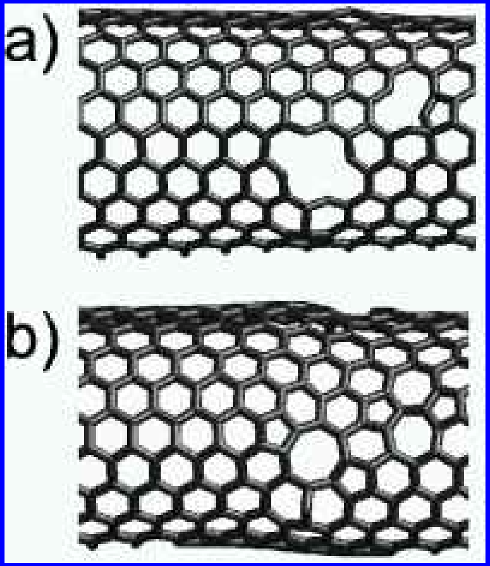

The second mechanism of the radiation defect annealing is the mending of vacancies through dangling bond saturation and by forming non-hexagonal rings and Stone-Wales defects.

P. M. Ajayan et al., Phys. Rev. Lett. **81** (98) 1437

Formation of topological defects

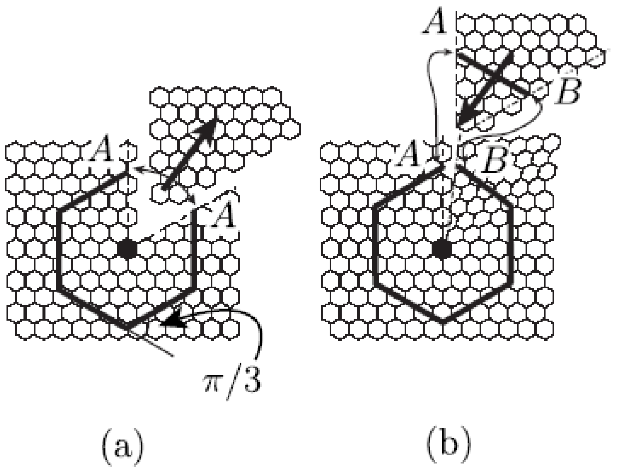

Fig. 1. (a) Formation of a $\pi/3$ wedge disclination and (b) a $-\pi/3$ wedge disclination. (a) Geodesic polygon around a $\pi/3$ disclination, and (b) that around a $-\pi/3$ disclination are also shown with bold lines. The points marked with A's and B's should be merged in each figure, so that the bold lines are closed.

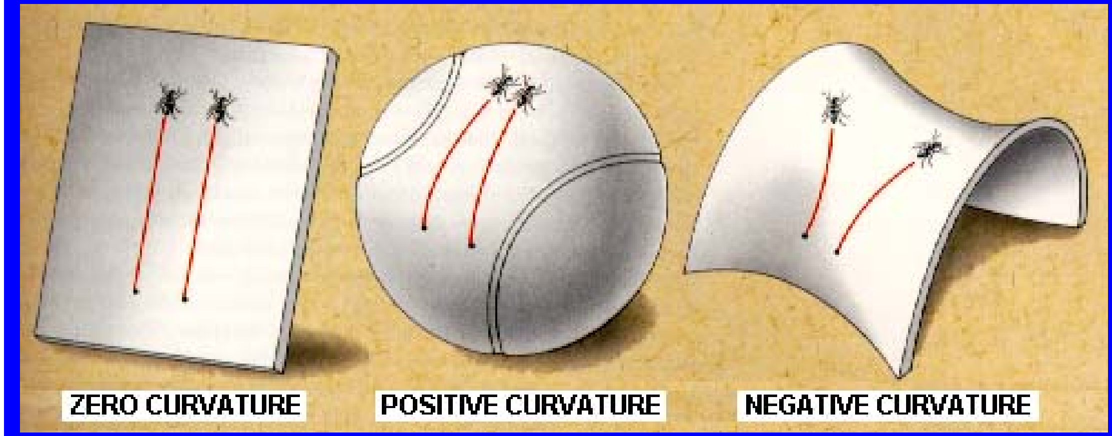

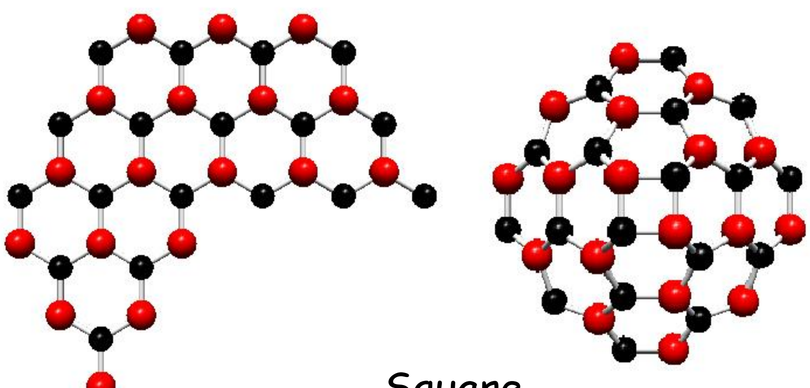

Square

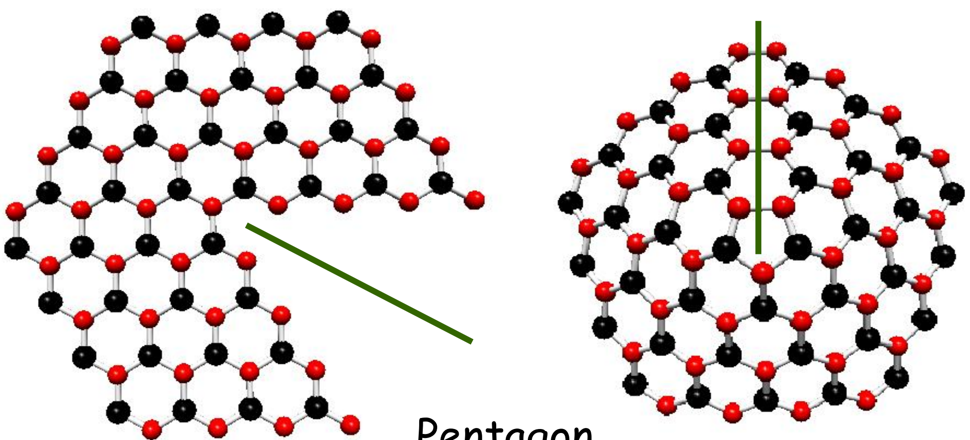

Pentagon

Odd-membered rings frustrate the lattice

The model for a single disclination

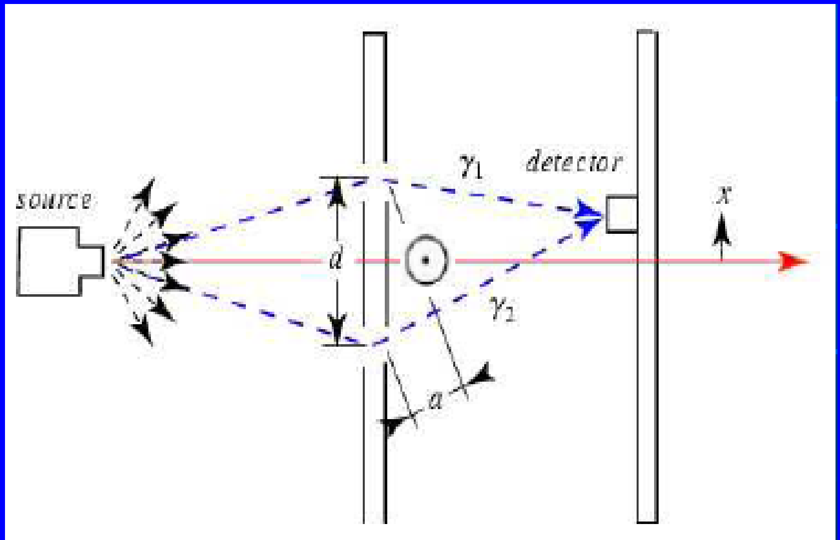

The Bohm-Aharonov effect

J. González, F. Guinea, and M. A. H. V., Phys. Rev. Lett. 69, 172 (1992)

$$\Psi_1 = \Psi_1^0 e^{-iS_1/h} \quad , \quad \Psi_2 = \Psi_2^0 e^{-iS_2/h}$$

$$(S_1 - S_2) = \frac{e}{c}\oint A.dx = \frac{e}{hc}\ \phi_0$$

A gauge potential induces a phase in the electron wave function

An electron circling a gauge string acquires a phase proportional to the magnetic flux.

Invert the reasonment: mimic the effect of the phase by a fictitious gauge field

$$H = \vec{\sigma}.(\vec{p} + ie\vec{A})$$

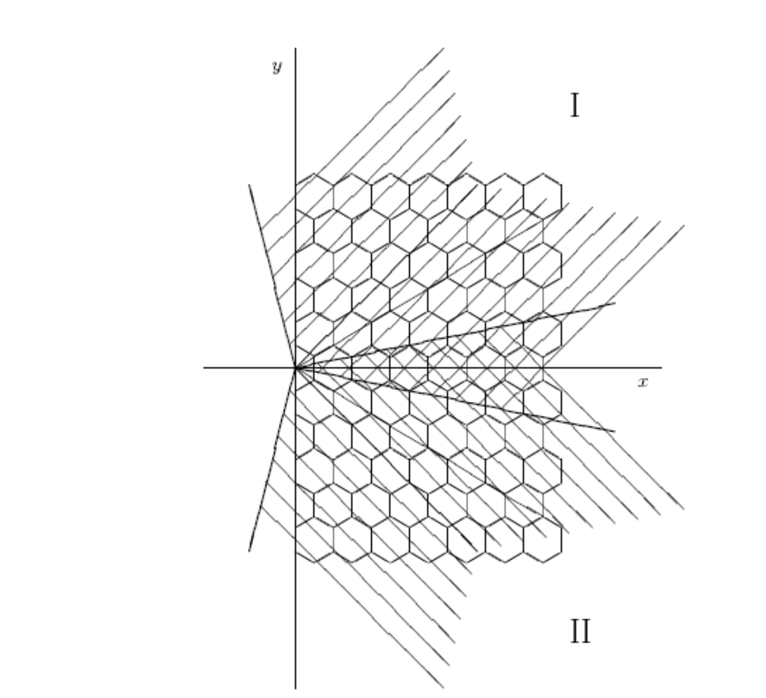

J. González, F. Guinea, and M. A. H. V., Nucl. Phys.B406 (1993) 771.

Substitution of an hexagon by an odd membered ring exchanges the amplitudes of the sublattices AB of grahene.

But it also exchanges the two Fermi points..

$$\Psi_\bullet = \sum_{i\,\bullet} e^{i\mathbf{k}\cdot\mathbf{r}_i} a_i^+ |O\rangle$$

$$\Psi_\circ = \sum_{i\,\circ} e^{i\mathbf{k}\cdot\mathbf{r}_i} a_i^+ |O\rangle$$

$$\mathcal{H}_+ = \begin{pmatrix} 0 & \gamma\sum_j e^{i\mathbf{k}\cdot\mathbf{u}_j} \\ \gamma\sum_j e^{i\mathbf{k}\cdot\mathbf{v}_j} & 0 \end{pmatrix} \qquad \lim_{a\to 0} \mathcal{H}_+/a = -\frac{3}{2}\gamma\, \boldsymbol{\sigma}^T\cdot\boldsymbol{\delta k}\Big|_{\mathbf{k}=(4\pi/3\sqrt{3})\mathbf{e}_x}$$

$$\mathcal{H}_- = \begin{pmatrix} 0 & \gamma\sum_j e^{-i\mathbf{k}\cdot\mathbf{u}_j} \\ \gamma\sum_j e^{-i\mathbf{k}\cdot\mathbf{v}_j} & 0 \end{pmatrix} \qquad \lim_{a\to 0} \mathcal{H}_-/a = \frac{3}{2}\gamma\, \boldsymbol{\sigma}^T\cdot\boldsymbol{\delta k}\Big|_{\mathbf{k}=-(4\pi/3\sqrt{3})\mathbf{e}_x}$$

Use a non-abelian gauge field

$$\vec{A} = \vec{A}_\alpha T^\alpha$$

For a pentagon

$$T = \begin{pmatrix} 0 & 1 \\ 1 & 0 \end{pmatrix}$$

Different types of disorder

Disorder can be included in the system by coupling the electrons to random gauge fields.

- Theory of localization in two dimensions *P. Lee*, *Ramakrishnan*, RMP'85
- Integer quantum Hall effect transitions *Ludwig*, *M. Fisher*, *Shankar*, *Grinstein*, PRB'94
- Disorder effects in d-wave superconductors *Tsvelik*, *Wenger*

$$H_{dis} = v_\Gamma \int d^2x\, \overline{\Psi}(x)\, \vec{\Gamma} \cdot \vec{A}\, \Psi(x)$$

Tipes of disorder: represented by the different possible gamma matrices.

$$\left.\begin{array}{ll} \gamma_0 & \text{Random chemical potential} \\ \gamma_{1,2} & \text{Random gauge potential} \\ I & \text{Random mass} \end{array}\right\}$$

Found previously in 2D localization and IQHT studies (no interactions, CFT techniques).

γ_5 **Topological disorder** $\Rightarrow$ **New, associated to the graphite system.**

The problem of including disorder and interactions is that CFT techniques can not be used.

Topological disorder

Topological disorder. Substitute some hexagons by pentagons and heptagons.

GGV
Nucl. Phys. B**406**, 771 (93)

Conical singularities: curve the lattice and exchange the A, B spinors.
Model: introduce a non-abelian gauge field which rotates the spinors in flavor space.

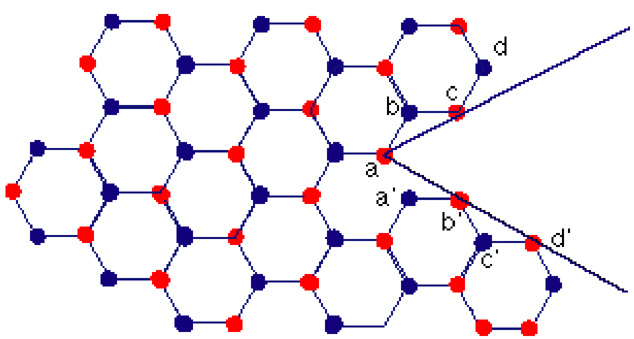

$\begin{pmatrix} \psi_A \\ \psi_B \end{pmatrix}$ Isospin doublet $\mathbf{A} \equiv \mathbf{A}^{(a)} \tau^{(a)}$; τ : Pauli matrices

$$A_\varphi = \frac{\varphi}{2\pi} \tau^{(2)} \quad ; \quad \varphi = \pi/2 \quad ; \quad e^{i \oint \mathbf{A}} = \begin{pmatrix} 0 & -1 \\ -1 & 0 \end{pmatrix}$$

GGV, Phys. Rev. B**63**, 13442 (01)

The combination of a pentagon and an heptagon at short distances can be seen as a dislocation⌦ vortex-antivortex pair.

Pentagon: disclination of the lattice.

Lattice distortion that rotates the lattice axis parametrized by the angle θ(**r**). It induces a gauge field:

$$\mathbf{A}(\mathbf{r}) = 3\nabla\theta(\mathbf{r}) \begin{pmatrix} 0 & -i \\ -i & 0 \end{pmatrix} .$$

Random distribution of topological defects described by a (non-abelian) random gauge field.

$$\langle \mathbf{A}(\mathbf{r}), \mathbf{A}(\mathbf{r}') \rangle = \Delta \delta^2(\mathbf{r} - \mathbf{r}') \ ;$$

Δ gives rise to a marginal perturbation which modifies the dimension of the fermion fields and enhances the density of states.
Short-range interactions enhanced.

$$2d_\psi - 1 = 1 - \frac{\Delta}{\pi} .$$

Inclusion of disorder in RG

T. Stauber, F. Guinea and MAHV, Phys. Rev. **B 71**, R041406 (05)

Disorder can be included in the RG scheme by coupling the electrons to random gauge fields.

$$H_{dis} = v_\Gamma \int d^2x\, \overline{\Psi}(x)\, \vec{\Gamma} \cdot \vec{A}\, \Psi(x)$$

$$\left\langle A_\mu(\mathbf{x}), A_\nu(\mathbf{y}) \right\rangle = \Delta \delta^2(\mathbf{x}-\mathbf{y})\delta_{\mu\nu}$$

A's are random in space and constant in time

$$\left\langle A(\mathbf{x}) \right\rangle = 0$$

Add new propagators and vertices to the model and repeat the RG analysis.

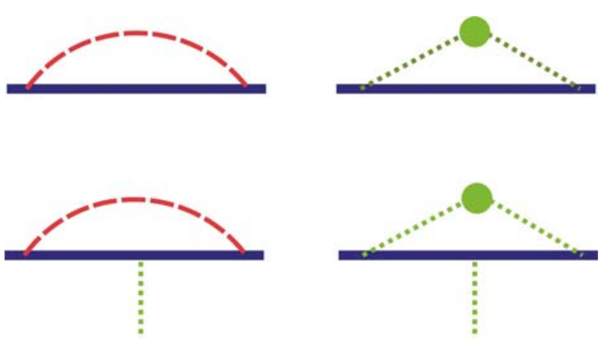

Affect the renormalization of the Fermi velocity, hence of g.

Renormalize the disorder couplings.

New diagrams at one loop

Electron propagator

Disorder line averaged

Photon propagator

Phase diagrams

RG flow equations can be encoded into a single parameter v_F

$$\frac{d}{dl}\frac{v_F^{eff}}{v_F} = \frac{1}{16\pi}\left[\frac{e^2}{v_F^{eff}} - \frac{\Delta}{2}\left(\frac{v_\Gamma^{eff}}{v_F^{eff}}\right)^2\right]$$

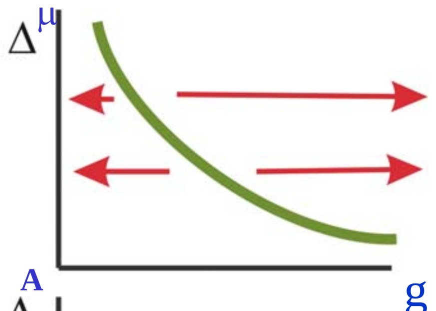

Random chemical potential

$\Gamma = \gamma^0 \quad \rightarrow \quad v_\mu = v_1$ (const)

Unstable fixed line

Divides the phase space in a strong and a weak coupling regime.

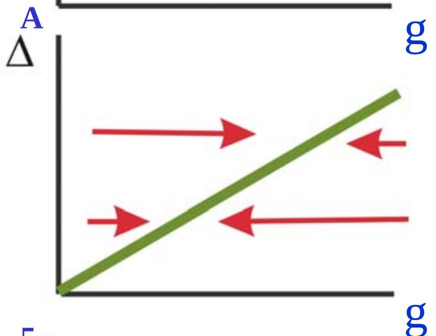

Random vector field

$\Gamma = \vec{\gamma} \quad \rightarrow \quad v_{\mathbf{A}} = v_F$

Line of fixed points

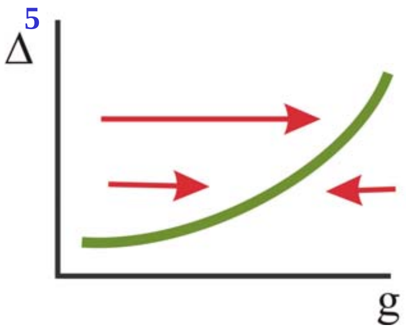

Topological disorder (or random mass)

$\Gamma = \gamma^5, \mathrm{I} \quad \rightarrow \quad v_m = v_F^2 / v_3$

Line of fixed points

New, non-trivial interacting phases

Topological Disorder

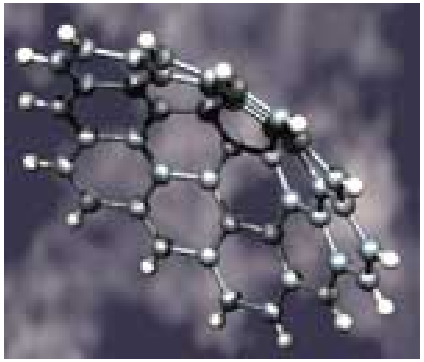

Pentagon: induces positive curvature

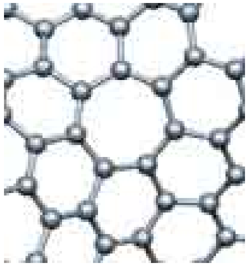

Heptagon: induces negative curvature

The combination of a pentagon and an heptagon at short distances can be seen as a dislocation of the lattice

Continuumm model for the spherical fullerenes

Promediate the curvature induced by the (12) pentagons and write the Dirac equation on the surface of a sphere.

To account for the fictitious magnetic field traversing each pentagon put a magnetic monopole at the center of the sphere with the appropriate charge.

$$i\sigma^a e_a^\mu \left(\nabla_\mu - iA_\mu\right)\Psi_n = \varepsilon_n \Psi_n \quad , \quad a,\mu = 1,2$$

$$\begin{aligned}
\nabla_\theta &= \partial_\theta \\
\nabla_\phi &= \partial_\phi - \frac{1}{4}\left[\sigma^1, \sigma^2\right] cos\theta \\
A_\theta &= 0 \\
A_\phi &= g\, cos\theta\, \tau^{(2)}
\end{aligned}$$

Spectrum

$$\varepsilon_J = \frac{\hbar v_F}{R}\sqrt{\left[J(J+1)\right] - l(l+1)} \quad J \geq l$$

Solving the problem in the original icosahedron much more difficult.
Want to model flat graphene with an equal number of pentagons and heptagons.

Generalization

A. Cortijo and MAHVcond-mat/060371

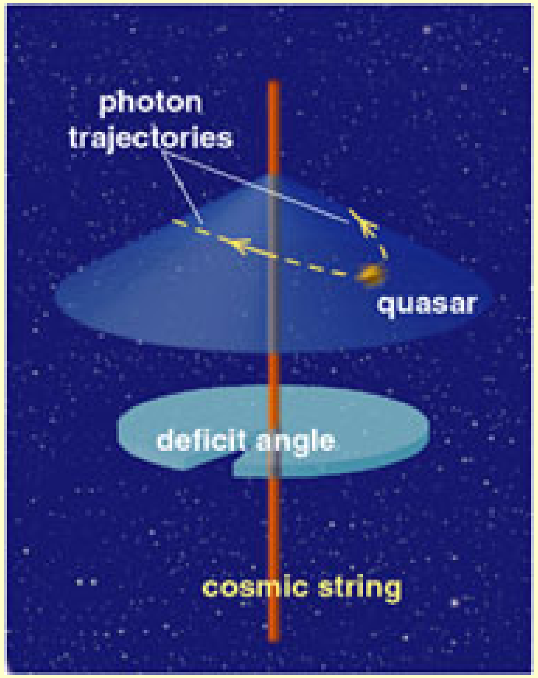

Cosmic strings induce conical defects in the universe. The motion of a spinor field in the resulting curved space is known in general relativity.

Generalize the geometry of a single string by including negative deficit angles (heptagons). Does not make sense in cosmology but it allows to model graphene with an arbitrary number of heptagons and pentagons.

Gravitational lensing: massive objects reveal themselves by bending the trajectories of photons.

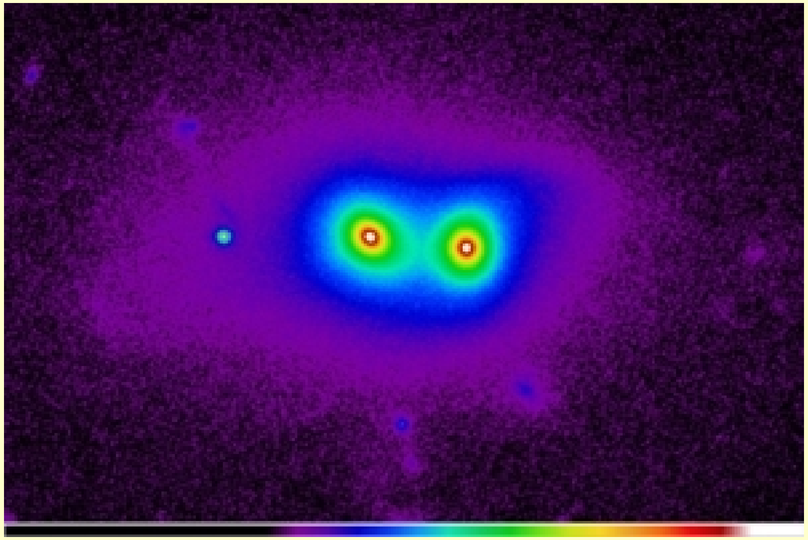

Capodimonte Sternberg Lens Candidate N.1

Cosmology versus condensed matter

NASA's Spitzer Space Telescope.

- G. E. Volovik: “The universe in a helium droplet”, **Clarendon press, Oxford 2000.**

- Bäuerle, C., *et al.* 1996. Laboratory simulation of cosmic string formation in the early universe using superfluid ^{3}He. *Nature* 382:332-334.

- Bowick, M., et al. 1994. The cosmological Kibble mechanism in the laboratory: String formation in liquid crystals. *Science* 236:943-945.

We play the inverse game: use cosmology to model graphene

The model

$$i\gamma^{\mu}(\mathbf{r})(\partial_{\mu}-\Gamma_{\mu})S_F(x,x')=\frac{1}{\sqrt{-g}}\delta^3(x-x')$$

Equation for the Dirac propagator in curved space.

$$ds^2=-dt^2+e^{-2\Lambda(x,y)}(dx^2+dy^2)$$

$$\Lambda(\mathbf{r})=\sum_{i=1}^{N}4\mu_i\log(r_i)\ ,\quad r_i=\left[(x-a_i)^2+(y-b_i)^2\right]^{1/2}$$

The metric of N cosmic strings located at $(a, b)_i$ with deficit (excess) angles μ_i.

$$N(\omega,r)=\mathrm{Im}\,TrS_F(\omega,r)$$

The local density of states

To first order in the curvature get

$$[i\gamma_{\mu}\partial_{\mu}-V(\omega,r)]S_F=\delta^2(\mathbf{x}-\mathbf{x}')$$

the equation for the propagator in flat space with a singular, long range potential

$$V(\omega,\mathbf{r})=2i\Lambda\gamma^0\omega+i\Lambda\gamma^j\partial_j+\frac{i}{2}\gamma^j(\partial_j\Lambda).$$

The result:

$$\delta N(\omega,\mathbf{r})=\frac{\mu}{2\pi^3 v_F^2}2\omega\Sigma_{i=1}^{N}\int dk\frac{J_0(\omega r_i)}{k^2}(4\omega^2-k^2)F(\omega,k),$$

$$F(\omega,r)=\left\{\begin{array}{l}\frac{-atanh\left(\frac{\sqrt{k^2-4\omega^2}}{k}\right)}{\sqrt{k^2-4\omega^2}},\ 4\omega^2<k^2\\ \frac{atan\left(\frac{k}{\sqrt{4\omega^2-k^2}}\right)}{\sqrt{4\omega^2-k^2}},\ 4\omega^2>k^2\end{array}\right\}.$$

A single disclination

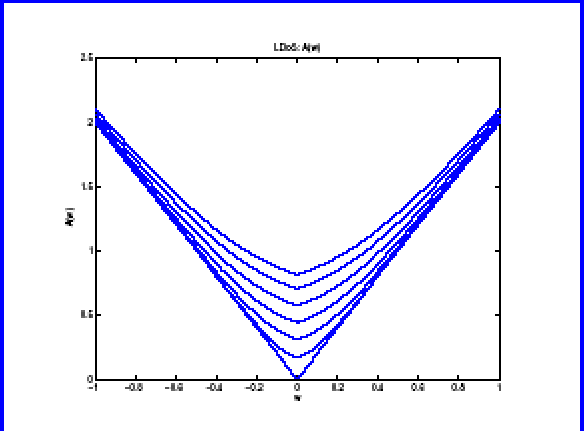

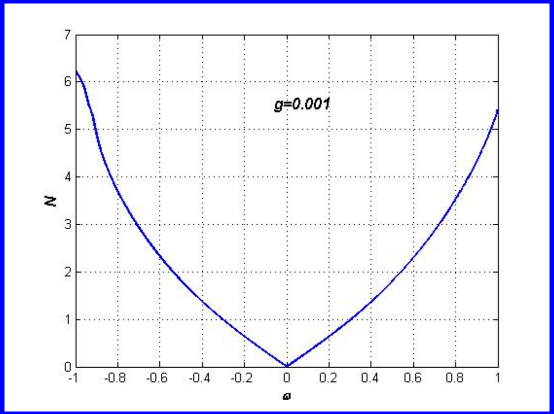

The total DOS at the Fermi level is finite and proportional to the defect angle for even membered rings.

Odd-membered rings break e-h symetry. DOS(Ef) remains zero.

Even-membered rings

Odd-membered rings

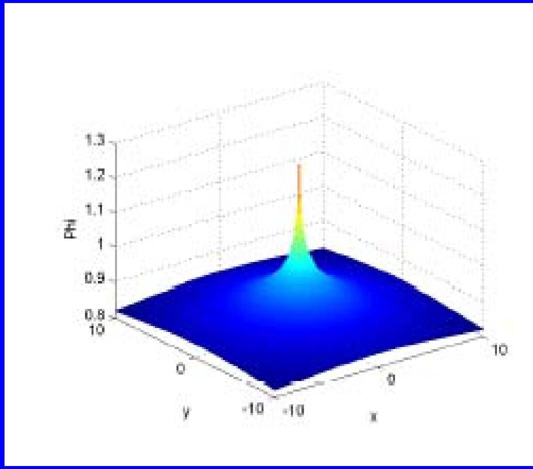

Electronic density around an even-membered ring

The zero energy states are peaked at the site of the defect but extend over the whole space. The system should be metallic.

The Fermi velocity is smaller than the free: competition with Coulomb interactions.

Several defects at fixed positions

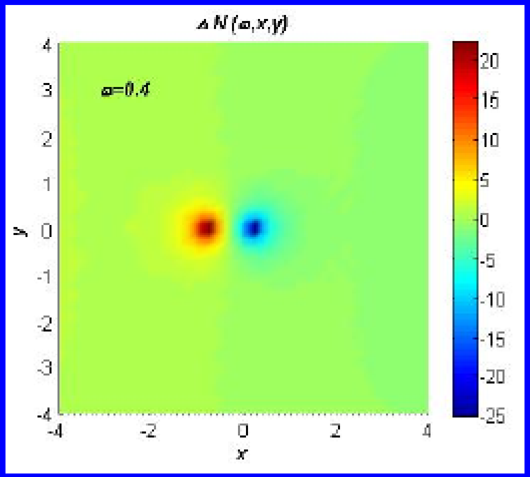

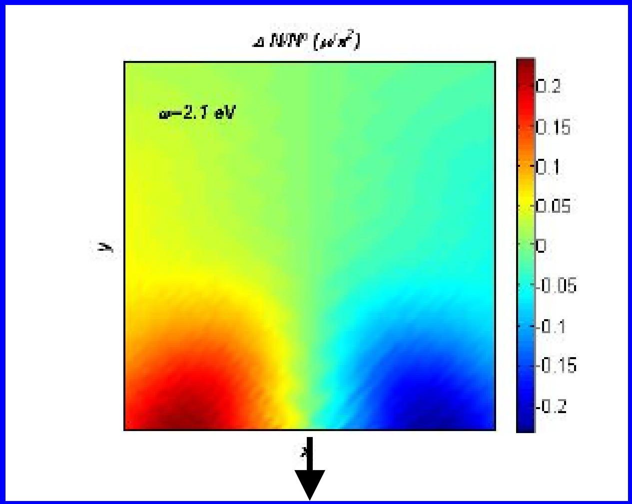

Pentagons (heptagons) attract (repell) charge.

Pentagon-heptagon pairs act as dipoles.

Local density of states around a hept-pent pair

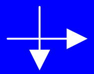

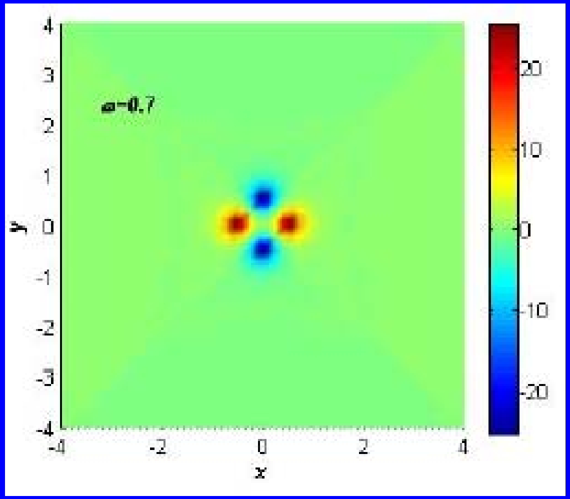

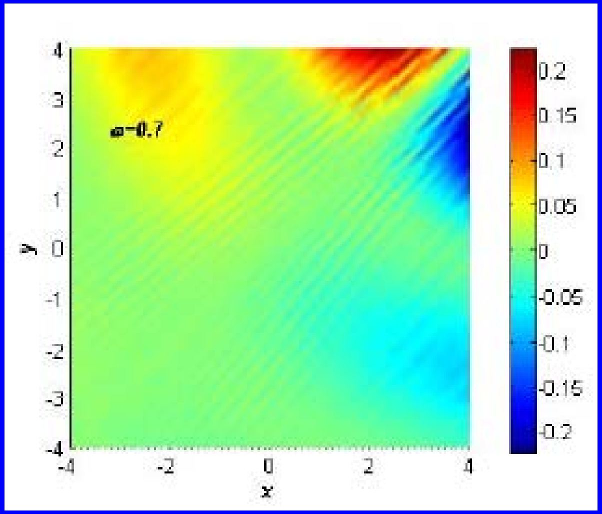

Local density of states around a Stone-Wales defect

Evolution with the energy

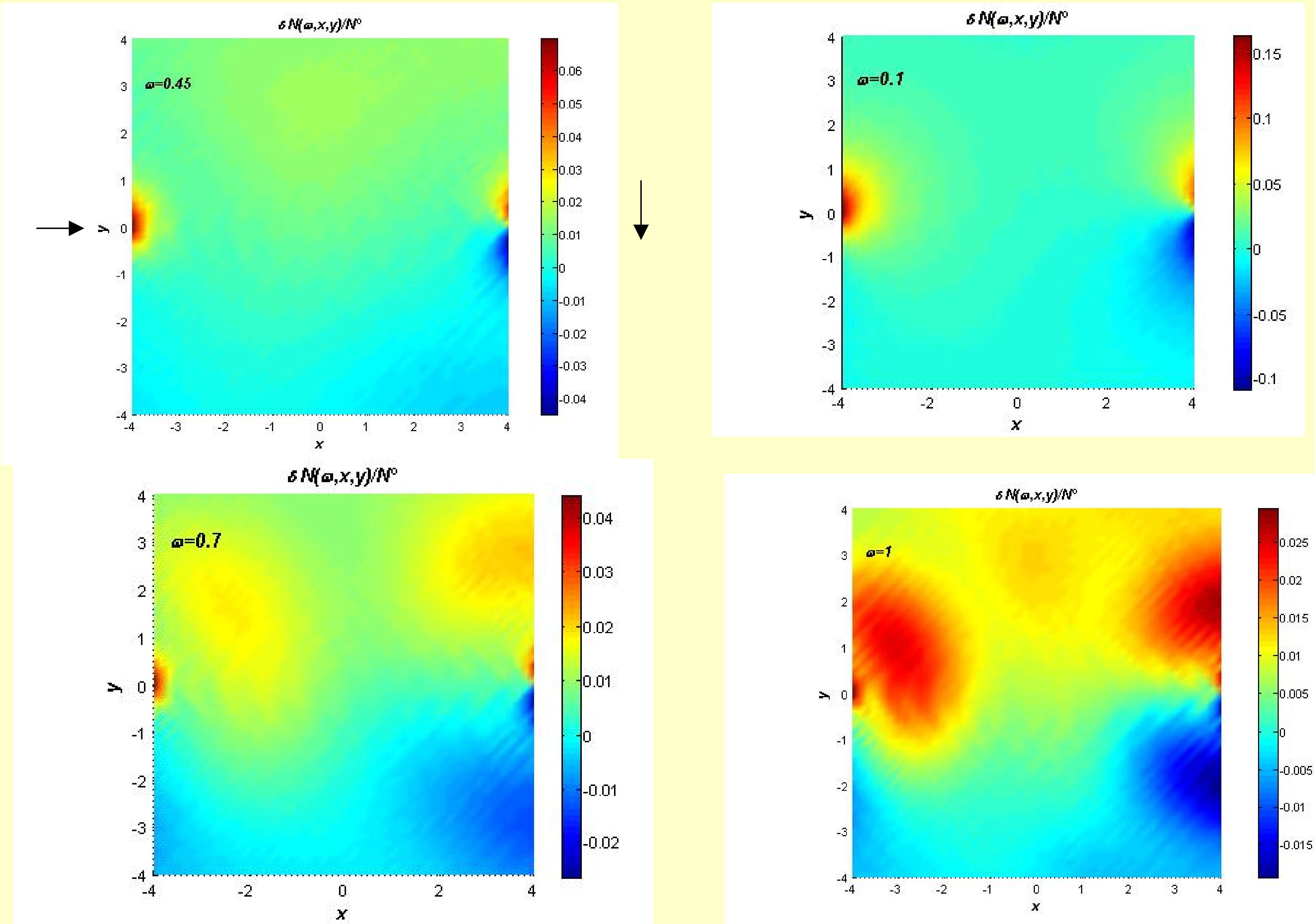

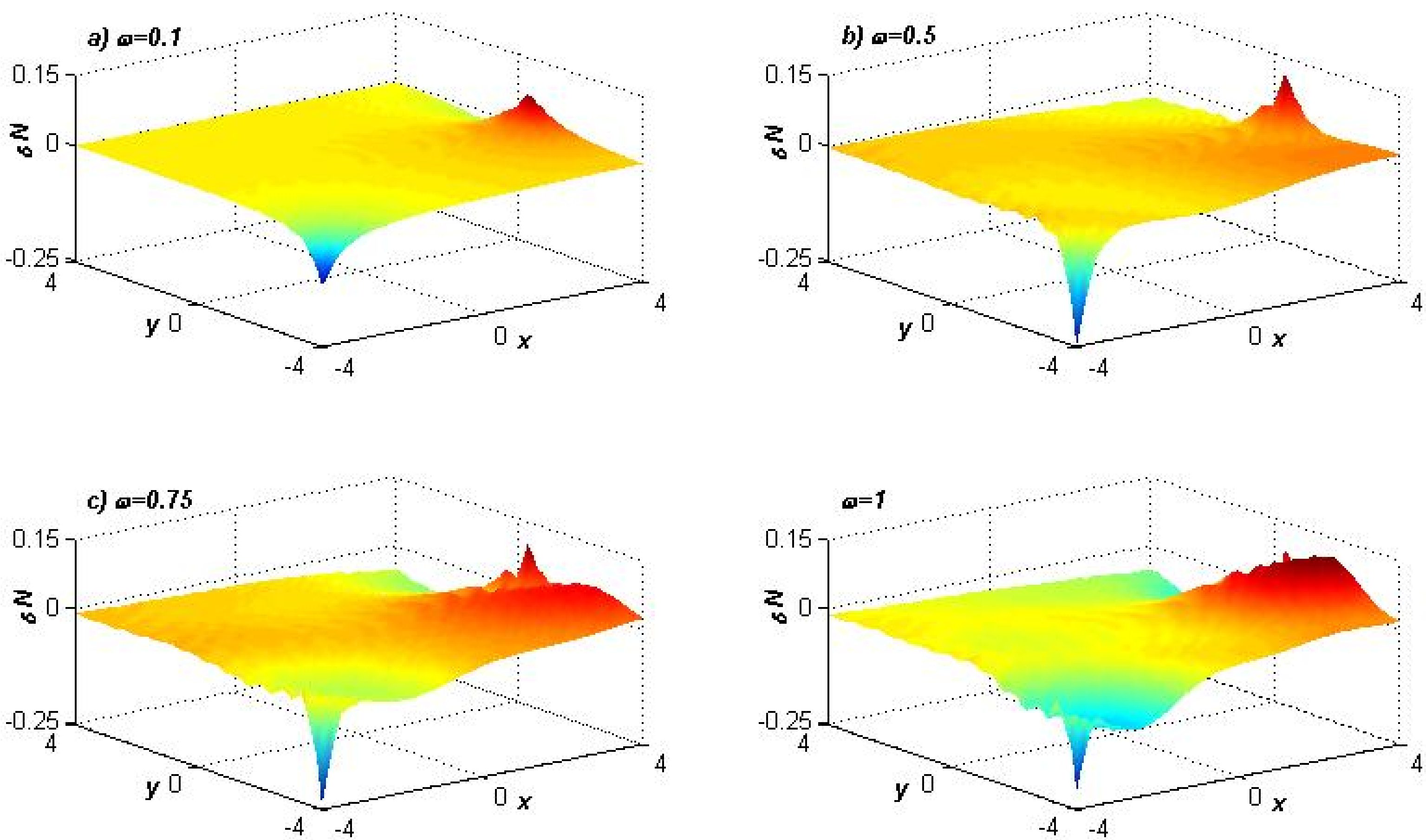

a) ω=0.1
b) ω=0.5
c) ω=0.75
ω=1
0.15
0
-0.25
δN
y
x
4
-4

Averaging over disorder

(Preliminary results)

$$S = \int d\vec{r}dt\bar{\Psi}iv_F(\gamma^\mu\partial_\mu)\Psi - \int d\vec{r}dt\bar{\Psi}iv_F(\Lambda(r)\gamma\nabla + \tfrac{1}{2}\gamma\nabla\Lambda(r))\Psi$$

$$< \Lambda(q)\Lambda(q') >= \frac{g}{q^2}\delta(q+q')$$

→ **unscreened singular interaction**

$$< \nabla^i\Lambda(q)\nabla^j\Lambda(q') >= g\delta^{ij}\delta(q+q')$$

→ **four-Fermi effective interaction**

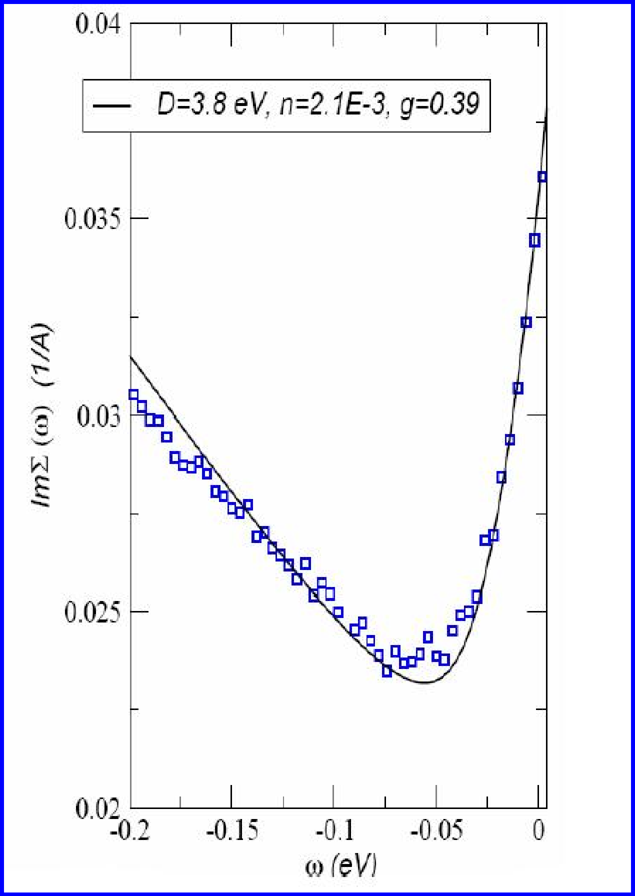

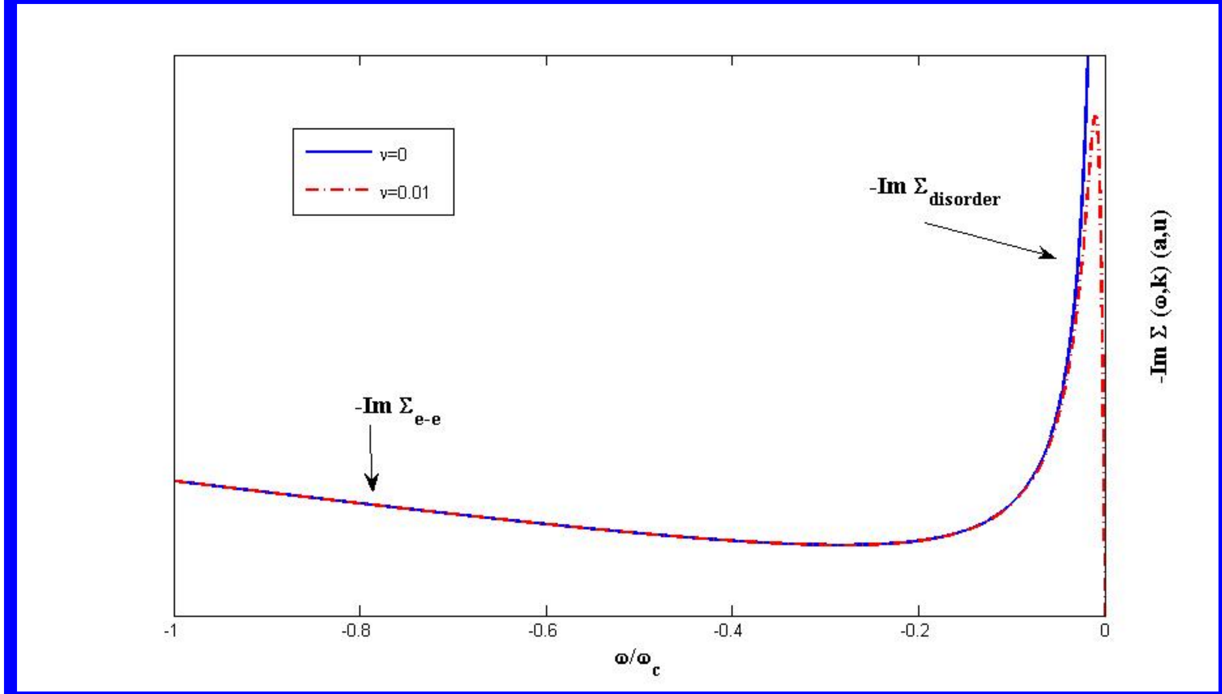

For small ω, Im Σ behaves as ~1/ω
For large ω the electron-electron Interaction dominates, but is modified by the effective local interaction:

Competition with Coulomb interactions

$$\mathrm{Im}\,\Sigma \sim \left(\frac{e^4}{\varepsilon_0^2 v_F^2} - \frac{g}{4\pi}\right)\omega$$

Conclusions and future

- Topological defects occur naturally in graphite and graphene.
- They induce long range interactions in the graphene system.
- Single conical defects enhance the metallicity of the system.
- A set of defects give rise to characteristic energy-dependent inhomogeneities in the local density of states that can be observed with STM and can help to characterize the samples.

- Localization (or not) of the states around the defects.
- Influence on ferromagnetism: interplay of DOS and Fermi velocity renormalization. RKKY with a disordered medium.
- Universal properties of a random distribution of defects.

A living curiosity:

Cell Division Program
Sergei Fedorov (Moscow) and
Michael Pyshnov (Toronto)

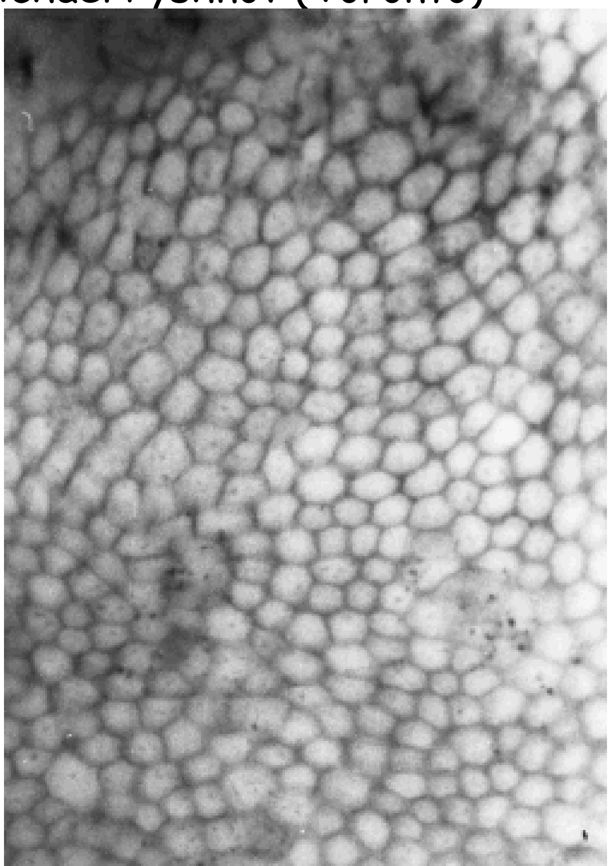

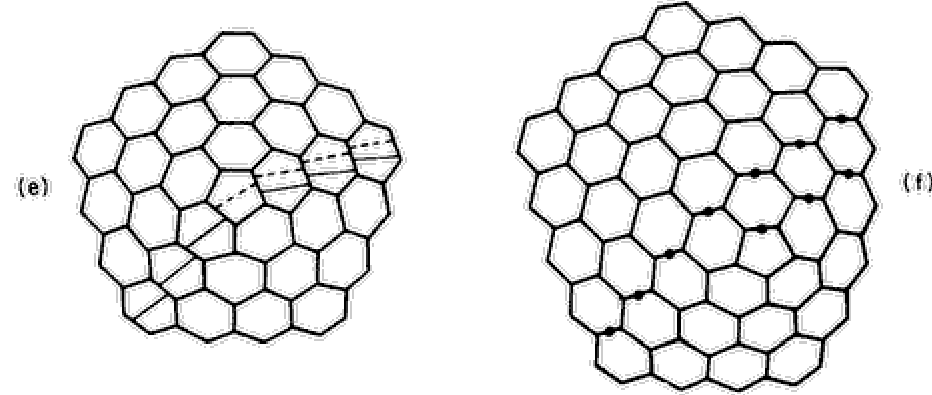

FIG. 4. Rules of cell division. (a) Division in the hexagonal row between pentagons. Emergence of the new division wave (dashed lines), when two division waves (thin solid approach the same pentagon from adjacent cells (c) and from non-adjacent cells (e). (b), The corresponding areas after division; sister cells are connected with dots. Note that three cells have divided twice and correspondingly in (f) two cell generations are connecte dots.

J. theor. Biol. (1980) 87, 189
Michael Pyshnov

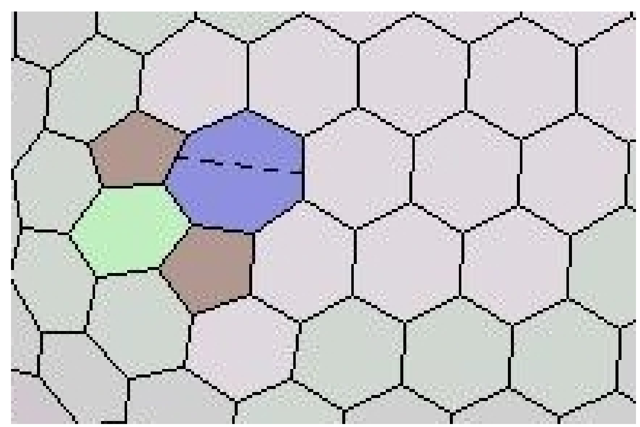

Surface of the epithelium of the villis.